

# IMPROVING THE MECHANICAL, THERMO-MECHANICAL PROPERTIES AND THERMAL CONDUCTIVITY OF CARBON FIBER/EPOXY BY INCORPORATING HALLOYSITE/CARBON NANOCOMPOSITES

Xueping Wu<sup>1,\*</sup>, Junshuai Zhao<sup>1</sup>, Xianlong Zhang<sup>1</sup>, Qi Shi<sup>1</sup>, Xiaolin Qi<sup>1</sup>, Yucheng Wu<sup>2</sup>

<sup>1</sup> School of Chemistry and Chemical Engineering, Hefei University of Technology, Hefei 230009, China. E-mail:18856957829@163.com

<sup>2</sup> School of Materials Science and Engineering, Hefei University of Technology, Hefei 230009, China

**Keywords:** Carbon fiber, Halloysite/carbon, Mechanical properties, Thermal conductivity, Thermo-mechanical properties

## ABSTRACT

Halloysite were combined with amorphous carbon via a hydrothermal route for halloysite/carbon (HNT/CS) nanocomposite synthesis in which the halloysite (HNT) was used as the template and chitosan (CS) as the carbon precursor at 180 °C for 24h [1]. carbon fiber/Epoxy-halloysite/carbon (CF/EP-HNT/CS) composites were fabricated via compression molding process. Results showed that there is a better synergistic effect between the HNT template and the coated carbon layer, which results in better dispersion and higher mechanical strength than each other. Moreover, the amino groups (-NH) in the carbon layer (hydrothermal carbonization of chitosan) on the HNT surface can improve the dispersion of HNT/CS in the epoxy resin, and provide a strong interactions with the epoxy resin system through a chemical bonding [2], the schematic illustration of chemical bonding between HNT/CS and epoxy resin is shown in Fig. 1. In addition, the better dispersion can enhance interface bonding and form a network structure [3]. Therefore, there are more effective load transfer and thermal transmission between epoxy matrix and reinforcements. The incorporation of HNT/CS-0.5 (in which the mass ratio of chitosan to halloysite was 0.5) resulted in 19.2% and 31.6% increases in the flexural strength and flexural modulus of the multiscale CF/EP laminates, respectively, with respect to the flexural strength and modulus of neat BF/EP laminates. A 20.4% increase was also recorded for the storage modulus of the multiscale CF/EP laminates relative to the neat CF/EP composites when introduced HNT/CS-0.5 in epoxy resin. Moreover, with the addition of HNT/CS-0.5, the thermal conductivity of the multiscale CF/EP laminates improved by 113% relative to the thermal conductivity of the neat CF/EP composites.

## 1 INTRODUCTION

In recent years, fiber-reinforced polymer (FRP) composites have a wide range of industrial applications, and the high performance are required, such as aerospace, automobiles, construction, and electrical insulators [4, 5]. Especially the carbon fiber-reinforced polymer, as a type of engineering materials which have an mature development recent years, and have a extensive application. This is mainly because carbon fiber possess specific properties highly, in particular, high stiffness , modulus

of elasticity and strength, which make carbon fiber as the reinforcing elements in the composite materials possess prodigious attraction [6-8].

However, owing to the intrinsic brittleness of epoxy matrix and weak carbon fiber/matrix interface, CF/EP composites has restricted applications to a great extent [7]. In order to improve these problems, there are two major methods: (i) surface treatment of carbon fibers, for example, fiber sizing and fiber coating [9], thermo-chemical treatment [10], liquid-phase chemical oxidation [11], ultraviolet generated ozone treatment (UV/O<sub>3</sub>) [12], etc.; (ii) modification of polymer matrix, i.e. the reinforcement of interface is accomplished by coordinated the properties of polymer matrix with fillers of chosen cautiously, such as inorganic nanoparticles [7, 13] and carbon-based materials, etc; the carbon-based materials include carbon nanotubes [14-19], carbon black (CB) [20] and graphene [21] etc. In the polymer matrix with different nanoreinforcements relative to conventional fiber-reinforced composites can reach to maximize the advantages of structural composites [22]. Ogasawara et al. [23] found that tensile strength and compression strengths increased 2–12% by adding 0.5% of fullerene into the epoxy matrix respectively, 60% enhancement in interlaminar fracture toughness by introduce the fullerene (0.1-1 wt%) into the epoxy matrix. Pathak AK [24] examined the enhancement of 25% of ILSS, while the flexural strength increases by 66%, flexural modulus increases by 72% at 0.3 wt% of graphene oxide dispersed in epoxy matrix, the enhancement was due to hydrogen type bonding and mechanical interlocking of graphene oxide with carbon fibers and epoxy resin. Vaganov et al. [25] has reported 40% enhancement in fracture toughness at 1.0 wt% CNTs in epoxy resin, while flexural strength and flexural moduli have a certain degree of increase, the increase in these result is certainly related to the bridging effect of the CNTs. Zhou YX et al. [26] shows that add 2.0 wt% clay into carbon fiber/epoxy composite showed the highest and significant improvement in the storage modulus and flexural properties. Although carbon nanotubes, carbon black and graphene etc have a better effect to improve the performance of composite material, they are expensive and the raw materials are not easy to get. In addition, there is cheap and available for nanoclay, but the composites which modified by nanoclay not be functional. We via a hydrothermal route for halloysite/carbon (HNT/CS) nanocomposite synthesis in which the HNTs were used as the template and chitosan (CS) as the carbon precursor at 180°C for 24h [1], the nanocomposites combine nanoclay with carbon-based materials successfully, in addition, the nanocomposites is very cheap , raw materials are easily obtained and possess simple technology process. In addition to the above, carbon fiber/epoxy composites modified with HNT/CS not only possess the higher mechanical properties, but also possess functionality.

In this work, we modify carbon fiber/epoxy composites with HNT/CS, HNT template and the coated carbon layer can achieve better synergistic effect, what's more important is that the amino groups (-NH) of the carbon on the HNT surface can improve the dispersion of HNT/CS in the epoxy resin, provide a strong interactions with the epoxy resin through a chemical reaction, thus, there are more effective load transfer between HNT/CS and epoxy resin [2]. The mechanical, thermo-mechanical properties and thermal conductivity of carbon fiber/epoxy composites was investigate in this study.

## 2 EXPERIMENTAL

### 2.1 Materials

The matrix was epoxy resin (E-51) which a commercial-grade diglycidyl ether of bisphenol A supplied by Bluestar Wuxi Petrochemical Co. Ltd. (Jiangsu, China). The 4, 4'-methylene dianiline (DDM) obtained from Sinopharm Group Co. Ltd. (Shanghai, China). The carbon fiber (woven, 200g/m<sup>2</sup>) was supplied by Weihai Tuozhan Fiber Co. Ltd. (Shangdong, China). The halloysite was

purchased from golden sun ceramics Co. Ltd. (Zhengzhou, China). The chitosan (CS), ammonium iron sulfate hexahydrate ( $\text{FeSO}_4 \cdot (\text{NH}_4)_2\text{SO}_4 \cdot 6\text{H}_2\text{O}$ ), acetone, and other reagents were of analytical grade were purchased from Sinopharm Group Co, Ltd.

## 2.2 Synthesis of the HNT/CS

The HNT/CS nanocomposites was synthesized by a typical procedure [1]. HNT, chitosan and  $\text{FeSO}_4 \cdot (\text{NH}_4)_2\text{SO}_4 \cdot 6\text{H}_2\text{O}$  was dispersed in 70 mL of distilled water under vigorous magnetic stirring to form a homogeneous dispersion for 2 h at room temperature. Then, the mixture was transferred to a Toflon-lined stainless steel autoclave with a volume capacity of 100 mL, sealed and maintained at 180 °C for 24 h. The next thing to do was cooled the autoclave to room temperature naturally, after that, the as-prepared nanocomposites was centrifuged at 8000rev/min, washed three times by double distilled water and ethanol, and then dried in an oven at 60 °C for 5 h. In this procedure, the mass ratios of chitosan to HNTs were set to 0.5, 1, and 2 to obtain HNT/CS with various carbon contents (i.e., HNT/C-0.5, HNT/C-1, and HNT/C-2), as shown in Table 1.

Sample	Mass ratio of chitosan to HNT	N(%)	C(%)	H(%)	S(%)
HNT/CS-0.5	0.5	1.71	12.01	2.37	2.02
HNT/CS-1	1	2.80	20.10	2.47	1.59
HNT/CS-2	2	4.56	32.22	4.59	1.28

Table 1 Elemental analysis of HNT/CS nanocomposites

## 2.3 Fabrication of the CF/EP-HNT/CS composites laminates

First of all, a certain of HNT, HNT/CS-x ( $x= 0.5, 1, 2$ ) was dispersed respectively in 15 mL of acetone by ultrasonic treatment for 1 h and mechanical stirring using a magnetic stirrer for 1 h, then, the mixture was introduced into epoxy resin and stirred for 12 h at room temperature. Afterword, degassing to remove the acetone of epoxy/acetone-HNT/CS mixture solution in a vacuum oven at 60 °C for 30 min. After that, the harder of DDM was introduced into the mixture solution, the mass ratio of epoxy to DDM was 100:27.

The mixture solution above was brushed onto specific dimensions of carbon fiber fabrics to prepare prepreps. Then, the laminates were transferred to the heating oven at 60°C for 1 h and remove the acetone completely in vacuum oven. Afterword, the laminates stacked on a self-made mold and cured in a hot pressing machine, The laminates were pre-cured at 80 °C for 2 h and further cured at 160 °C for 4 h under a pressure of 1 MPa. The contents of all nanoreinforcements was 3wt% based on the nanocomposites matrix.

## 2.4 Characterizations of multiscale composites

Three-point bending tests in accordance with ASTM D 790 were performed using a universal testing machine (SANS CMT-4102, Shenzhen, China). The sample size was 70 mm × 12.7 mm × 2.5 mm, and the ratio of span length to thickness is 16:1. In addition, the constant crosshead speed of 1 mm/min at room temperature to ensure the reliability of test results.

SEM (JSM-6700F) was used to observe the fracture surfaces of the composites after being subjected to a flexural test at an operating voltage of 10 kV. The fracture surfaces was pre-chilled in liquid nitrogen, and coated with aurum sputter.

Dynamic mechanical analysis was performed using a dynamic mechanical analyzer (DMA, Q-800, TA Instrument, USA) to investigate the storage moduli and the glass transition temperatures ( $T_g$ ) of the multiscale laminates. Treatment conditions included a frequency of 1Hz and a temperature range of 25-230°C with 5°C/min of temperature ramp. The specimen dimensions was 40 mm × 15 mm × 2.5 mm.

The through-thickness thermal conductivity experiments were conducted at temperatures of 25 °C with the use of the LFA 457Micro Flash laser in an air atmosphere. The through-thickness thermal conductivities ( $\lambda$ ) of the multiscale BFRP laminates with and without nanoreinforcements were calculated:

$$\lambda = \alpha \rho C_p \tag{1}$$

where  $\alpha$  is the thermal diffusivity,  $\rho$  is the bulk density of the specimen, and  $C_p$  is the specific heat capacity obtained from DSC measurements.

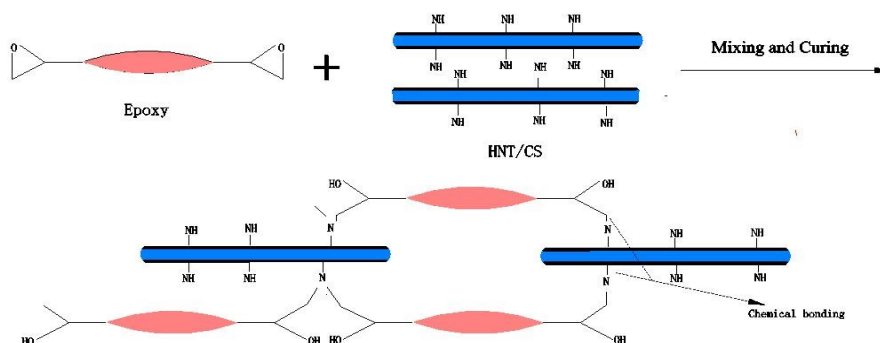


Fig.1. Schematic illustration of the chemical bonding between epoxy matrix and HNT/CS

### 3 RESULTS AND DISCUSSION

#### 3.1 Characterization of HNT/CS

Fig.2 shows the XRD patterns of natural HNT, hydrothermally treated chitosan and the HNT/CS nanocomposites. As for the halloysite, The peak at  $2\theta = 11.8^\circ, 20.0^\circ, 24.7^\circ, 35.0^\circ, 54.5^\circ,$  and  $62.5^\circ$  are indexed to the characteristic reflections of halloysite, which matches well with halloysite crystal structure [JCPDSNo. 29-1487], the reflection at  $2\theta = 26.7^\circ$  reveals that halloysite contains minor quartz [27]. The HNT/CS have the similar XRD patterns, which suggest that the crystal structure of halloysite is not destroyed after hydrothermally treated. Furthermore, a weak and broad diffraction peak between  $20^\circ$  and  $30^\circ$  is assigned to the amorphous carbon, indicating that the chitosan molecules have polymerized and successively carbonized as carbon.

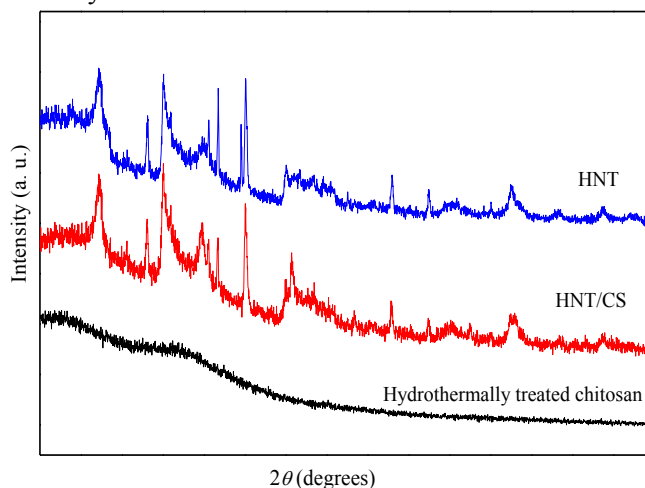


Fig.2. X-ray diffraction patterns of HNT clay, hydrothermally treated chitosan and HNT/CS nanocomposite

Fig 3 shows the transmission electron microscopy (TEM) images of HNT/CS nanocomposites, For the HNT, the inner diameters range from 10 nm to 30 nm, the outer diameters range from 50 nm to 100 nm, and lengths vary from 0.5  $\mu\text{m}$  to 1  $\mu\text{m}$  [28]. After hydrothermal treatment of halloysite and chitosan, chitosan carbonized on the HNTs surface and formed a carbon layer with a thickness of approximately 10nm (HNT/C-1). The energy-dispersive spectroscopy spectra (Fig. 3c) of the selected area in Fig. 3b show the elemental components of the carbon coating layer on the HNT surface. These indicate that the carbonaceous matter were formed on the external templates by the HNT process.



Fig.3. Transmission electron microscopy (TEM) (a, b) and EDS (c) images of HNT/CS nanocomposites

The FTIR spectra for the HNT, hydrothermally treated chitosan and HNT/CS are shown in Fig. 4. For the HNT, the bands occurred at  $3440\text{cm}^{-1}$  and  $1640\text{cm}^{-1}$  are due to O–H and N–H [29]. The peak of  $1035\text{cm}^{-1}$  and  $1093\text{cm}^{-1}$  indicate the Si–O and (Mg Al)–O stretching vibration respectively. The bands at  $3692\text{cm}^{-1}$  and  $3615\text{cm}^{-1}$  are attributed to O–H stretching of innersurface hydroxyl and inner hydroxyl groups respectively [30]. The signals at  $688\text{cm}^{-1}$  and  $534\text{cm}^{-1}$  correspond to perpendicular Si–O stretching and deformation of Al–O–Si, respectively [28]. For the hydrothermally treated chitosan nanocomposite, the peak at  $3440\text{cm}^{-1}$  is attributed to N–H and O–H stretching vibration [29]. The signals of  $2924\text{cm}^{-1}$  and  $2855\text{cm}^{-1}$  indicates the C–H stretching bands of  $-\text{CH}_2$  and  $-\text{CH}_3$ , respectively [28]. The band at  $1653\text{cm}^{-1}$  is assigned to the stretching vibration of amides and C=C stretching vibration of alkenes [31]. The peak at  $1602\text{cm}^{-1}$  is due to amino band. The peak at  $1386\text{cm}^{-1}$  and  $1323\text{cm}^{-1}$  correspond to C–N stretching bands. For the HNT/CS nanocomposites, there are several new bands, including  $2924\text{cm}^{-1}$  and  $2855\text{cm}^{-1}$  of C–H stretching bands of  $-\text{CH}_2$  and  $-\text{CH}_3$ , and  $1386\text{cm}^{-1}$  correspond to C–N stretching vibration. These results indicates that the HNT clay had been modified by the functional carbonaceous species successfully.

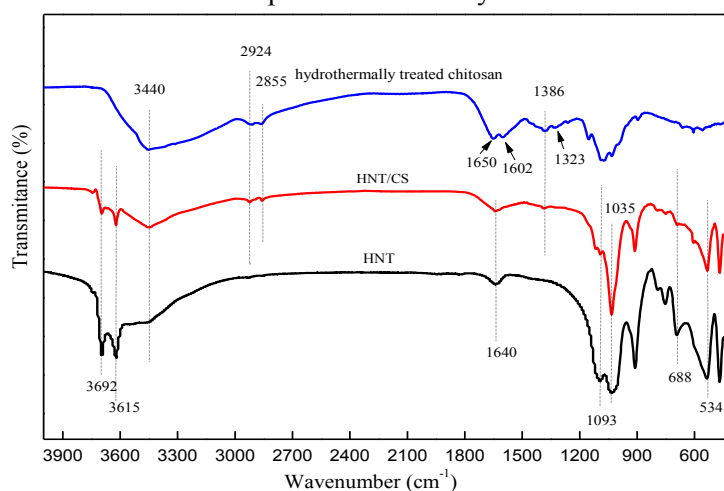


Fig. 4 FT-IR spectra of HNT, hydrothermally treated chitosan and HNT/CS nanocomposites

### 3.2 Morphological characteristics of the fracture surfaces

SEM images examination of the fracture surfaces of the neat CF/EP (Fig. 5a and b), CF/EP-HNT (Fig. 5c and d) and CF/EP-HNT/C-0.5 (Fig. 5e and f) composites. Fig. 5a shows that the fracture of the neat BF/EP laminates was relatively clean, and only few epoxy residues are found on the fiber surface because of the weak interface between carbon fiber and epoxy. In addition, debonding between carbon fiber and epoxy resin due to weak interfacial bonding is also clearly observable in Fig. 5b. carbon fiber is relatively harmonized with epoxy after adding HNT to CF/EP composites (Fig. 5c), many epoxy residues exist between the fibers, and fewer fibers were pulled out. In Fig. 5d, the bonding between carbon fiber and epoxy is improved than neat CF/EP composites clearly. As shown in Fig. 5e, the fibers in CF/EP-HNT/CS-0.5 are more harmonized with epoxy matrix, and more epoxy residues exist between the carbon fibers, fewer fibers are pulled out. In addition, a better bonding between the fiber and epoxy resin is shown in Fig. 6f especially. Such findings indicate a better improve interfacial interactions between carbon fiber and epoxy when add HNT/CS-0.5 to CF/EP composites, and stress could be effectively transferred from the epoxy matrix to carbon fibers.

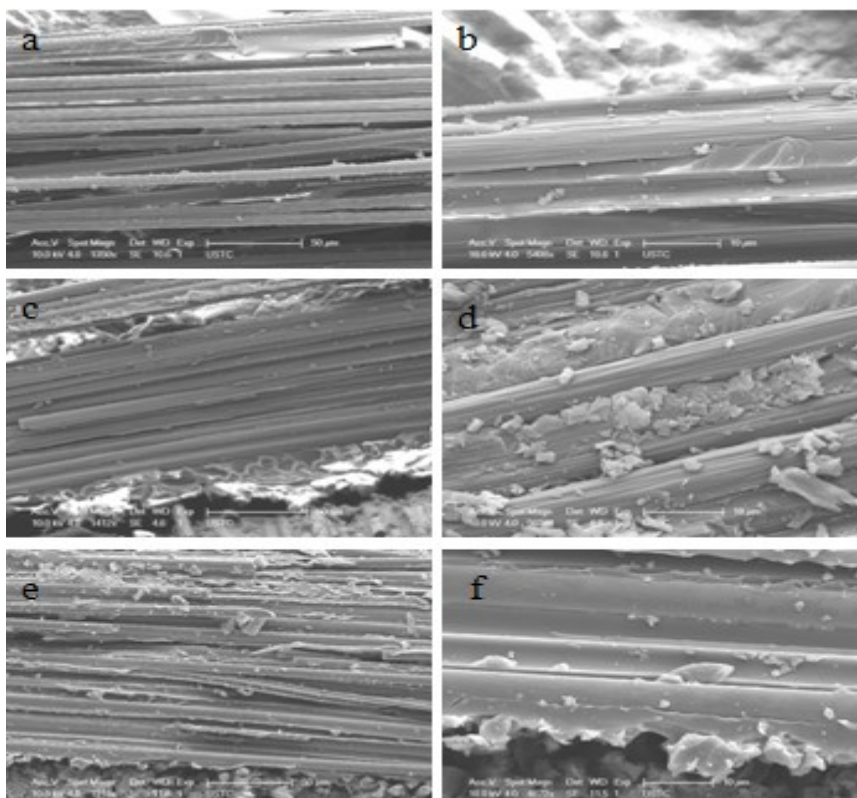


Fig.5. SEM images of the fracture surfaces of the neat CF/EP (a, b), CF/EP-HNT Laminates (c, d), CF/EP-HNT/CS-0.5 laminates (e, f)

### 3.2 Mechanical properties

The flexural properties of CF/EP, CF/EP-HNT, CF/EP-HNT/CS composites are plotted in Fig.6. For the CF/EP composites, the flexural strength and modulus are 508.4MPa and 32.5GPa, respectively. The addition of HNT and HNT/CS both have a obvious increase. At 3wt% HNT/CS-0.5, the composites show a 19.2% increase in flexural strength, and 31.6% increase in flexural modulus.

We can also found that the increase of adding HNT/CS to CF/EP is more effect than adding HNT for flexural properties. On the one hand, there is a better synergistic effect between the HNT template and the coated carbon layer, which results in better dispersion and higher mechanical strength than each other. On the other hand, the amine groups of the carbon (hydrothermal carbonization of chitosan) on the HNT surface can provide a strong interactions with the epoxy resin system through a chemical reaction [2], achieve more effective load transfer, the schematic illustration of chemical bonding between HNT/CS and epoxy resin as show Fig.1. Moreover, the strong interactions with HNT/CS and epoxy resin can avoided the agglomeration of HNT/CS due to physical factors, prevent stress concertration. In addition, the better dispersion can enhance interface bonding and form a network structure [3]. Therefore, there are more effective load transfer between epoxy matrix and reinforcements.

When increase the content of carbon on HNT surface, there are lower flexural properties, the main reason is that with increasing carbon contents on the HNT surface, which tend to agglomerate in the epoxy resin, thereby decreasing the surface area for interfacial adhesion, and decreasing the free volume for particles to move around [32, 33]. The aggregated particles lead to the formation of stress convergence points or as crack initiation sites [34], thus leading to lower flexural properties.

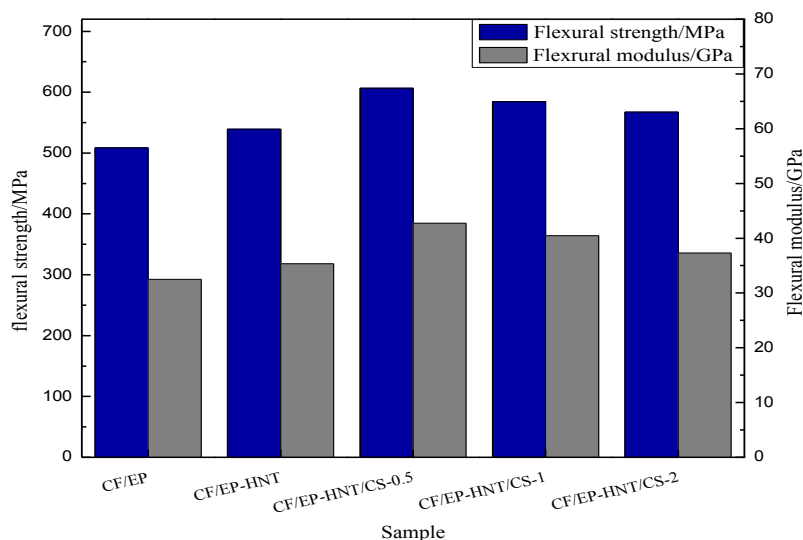


Fig.6. Flexural strength and modulus of CF/EP, CF/EP-HNT and CF/EP-HNT/CS composites

### 3.4 Dynamic mechanical analysis(DMA)

The effects of nanoreinforcements on the thermal properties of the CF/EP composites are investigated by comparing the storage modulus and  $\tan\delta$ . The numerical value of storage modulus and  $\tan\delta$  for CF/EP, CE/EP-HNT, CF/EP-HNT/CS composites at 3wt% loading of nanoreinforcements are given in Fig. 7 and Fig. 8.

The storage modulus is an important property to assess the load bearing capacity of composites material [7]. Fig.7 shows the storage modulus as a function of temperature for composites containing different nanoreinforcements. As the temperature increased, the storage modulus decreased, and then, there are a sharp decline in the glass transition region. This phenomenon is due to the increase in the molecular mobility of the polymer chains above  $T_g$  [7, 35]. In addition, the decrease of the CF/EP-HNT/CS and CF/EP-HNT composites were less than neat CF/EP composites in the modulus at the glass transition region. Especially for the composites with HNT/CS-0.5, there are a maximum increase related to CF/EP, and the storage modulus was enhanced by 20.4% at 220°C. HNT/CS-0.5 can achieve the better dispersion in epoxy resin, as discussed above, the better dispersion can improve storage modulus [3]. And then the better dispersion can also increase the contact area between nanofillers and epoxy resin. Moreover, the strong interactions of HNT/CS containing a certain amount

of -NH with the epoxy resin through a chemical bonding can achieve effective load transfer between nanoreinforcements and epoxy resin, thereby enhance the storage modulus of composites.

Fig.8 show the  $\tan\delta$  values of the composites, the peak position of  $\tan\delta$  is the glass transition temperature ( $T_g$ ). The  $T_g$  value of neat CF/EP is 202°C, with the containing HNT and HNT/CS-0.5, the  $T_g$  are 194°C and 199°C respectively, both of them show lower  $T_g$  than neat CF/EP. This result can be explained that unreacted molecular segments cause inhomogeneities from regions of varying crosslink density, the inhomogeneities break the regular crosslinking between epoxy resin and hardener [36]. However, the addition of HNT/CS-0.5 in the CF/EP composites have a higher value of  $T_g$ , compared with add HNT to CF/EP composites, this because the-NH of HNT/CS can participate the curing reaction of epoxy resin, enhance the crossing densities of epoxy. In addition, the HNT/CS induce improve interfacial strength between the HNT/CS and epoxy resin through chemical bonding, which hindrance to epoxy molecules mobility around the HNT/CS [37]. Thereby, the thermal stability (storage modulus and  $\tan\delta$ ) of the CF/EP-HNT/CS-0.5 composite is better than that of the CF/EP-HNT composite.

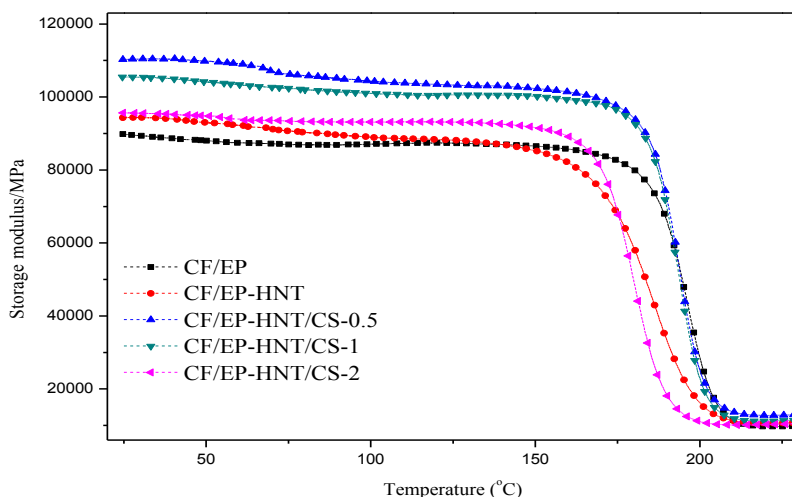


Fig. 7. Storage modulus of CF/EP, CF/EP-HNT and CF/EP-HNT/CS composites

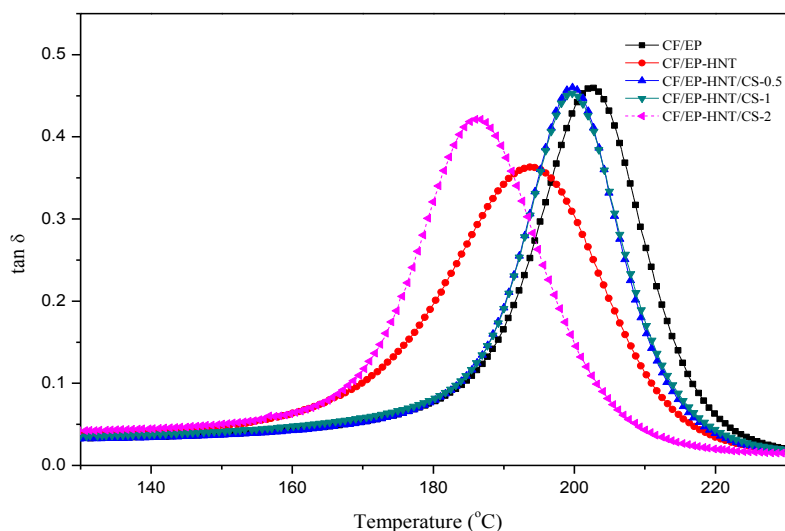


Fig. 8.  $\tan\delta$  of CF/EP, CF/EP-HNT and CF/EP-HNT/CS composites

### 3.5 Thermal conductivity

Fig. 9 presents the thermal conductivity variation of CF/EP composites containing different

nanofillers. It can be seen that when introduce HNT and HNT/CS into CF/EP nanocomposites, there are 50% and 113% increment in the thermal conductivity relate to neat CF/EP nanocomposites, respectively. Organic/inorganic composites mainly to transfer heat by phonons, the addition of HNT and HNT/CS are form of phonons conduction pathway in epoxy resin, thus enhance the thermal conductivity of composites. Otherwise, there are more effective when add HNT/CS to epoxy resin than add HNT. On the one hand, there is a certain thickness of carbon layer on HNT surface, carbon-based material possess higher thermal conductivity relate to silicate clay [38-40], in other words, HNT/CS possesses relatively high thermal conductivity than silicate clay, so HNT/CS can achieve effective thermal transmission in epoxy resin than nanoclay. On the other hand, HNT/CS have stronger interfacial bonding with epoxy resin though chemical reaction (as show in Fig. 1), the strong interfacial bonding can reduce phonon scattering and lower interfacial thermal resistance between HNT/CS and epoxy resin, thus, achieve more effective thermal transmission [41]. The strong interactions with HNT/CS and epoxy resin can avoided the agglomeration of HNT/CS due to physical factors, enhance the dispersion of HNT/CS in epoxy resin. A better dispersion can form high thermal conductivity pathway through form a better reticular structure, which results in an effective heat transfer and ultimately yielding the high thermal conductivity of CF/EP-HNT/C-0.5.

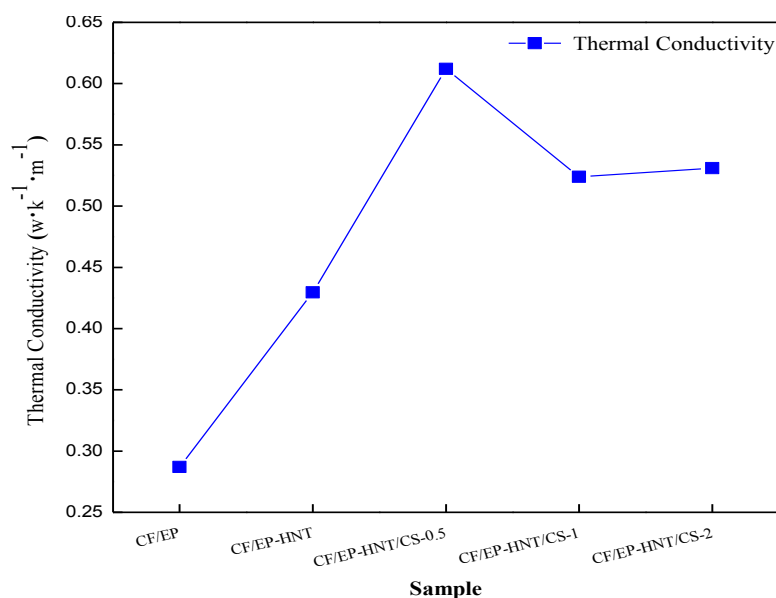


Fig.9. Thermal conductivity of CF/EP, CF/EP-HNT and CF/EP-HNT/CS composites

#### 4 CONCLUSIONS

The effect of HNT/CS nanocomposites on mechanical, thermo-mechanical properties and thermal conductivity were investigated in this work. At 3wt% HNT/CS, the flexural strength and modulus of nanocomposites are resulted in 19.2% and 31.6% increment related to neat CF/EP nanocomposites, a negative effect on flexural properties by increasing of the carbon contents on the HNT surface. when introduce HNT/CS into CF/EP nanocomposites, there is 20.4% increase in storage modulus relate to neat CF/EP nanocomposites, and 113% increase in thermal conductivity. The improved mechanical, thermo-mechanical properties and thermal conductivity of the CF/EP-HNT/CS composites were due to the better dispersion and strong interfacial interactions between HNT/CS and epoxy resin in the CF/EP composites.

#### ACKNOWLEDGEMENTS

This work was supported by Ministry of Science and Technology of Anhui Province (No. J2014AKKG0002).

## REFERENCES

- [1] Q. Zhou, Q. Gao, W. Luo, C. Yan, Z. Ji, P. Duan, One-step synthesis of amino-functionalized attapulgite clay nanoparticles adsorbent by hydrothermal carbonization of chitosan for removal of methylene blue from wastewater, *Colloids and Surfaces A: Physicochemical and Engineering Aspects*, **470**, 2015, pp. 248-257.
- [2] J. Cha, S. Jin, J.H. Shim, C.S. Park, H.J. Ryu, S.H. Hong, Functionalization of carbon nanotubes for fabrication of CNT/epoxy nanocomposites, *Materials & Design*, **95**, 2016, pp. 1-8.
- [3] K.C. Etika, L. Liu, L.A. Hess, J.C. Grunlan, The influence of synergistic stabilization of carbon black and clay on the electrical and mechanical properties of epoxy composites, *Carbon*, **47**, 2009, pp. 3128-3136.
- [4] A.R. Abu Talib, A. Ali, M.A. Badie, N. Azida Che Lah, A.F. Golestaneh, Developing a hybrid, carbon/glass fiber-reinforced, epoxy composite automotive drive shaft, *Materials & Design*, **31**, 2010, pp. 514-521.
- [5] I.D.G. Ary Subagia, Y. Kim, L.D. Tijing, C.S. Kim, H.K. Shon, Effect of stacking sequence on the flexural properties of hybrid composites reinforced with carbon and basalt fibers, *Composites Part B: Engineering*, **58**, 2014, pp. 251-258.
- [6] S.H. Han, H.J. Oh, H.C. Lee, S.S. Kim, The effect of post-processing of carbon fibers on the mechanical properties of epoxy-based composites, *Composites Part B: Engineering*, **45**, 2013 pp. 172-177.
- [7] Y. Ye, H. Chen, J. Wu, C.M. Chan, Evaluation on the thermal and mechanical properties of HNT-toughened epoxy/carbon fibre composites, *Composites Part B: Engineering*, **42** 2011, pp. 2145-2150.
- [8] B. Yu, Z. Jiang, X.-Z. Tang, C.Y. Yue, J. Yang, Enhanced interphase between epoxy matrix and carbon fiber with carbon nanotube-modified silane coating, *Composites Science and Technology*, **99**, 2014, pp. 131-140.
- [9] X. Yuan, B. Zhu, X. Cai, J. Liu, K. Qiao, J. Yu, Optimization of interfacial properties of carbon fiber/epoxy composites via a modified polyacrylate emulsion sizing, *Applied Surface Science*, **401**, 2017, pp. 414-423.
- [10] F. Vautard, S. Ozcan, H. Meyer, Properties of thermo-chemically surface treated carbon fibers and of their epoxy and vinyl ester composites, *Composites Part A: Applied Science and Manufacturing*, **43**, 2012, pp. 1120-1133.
- [11] E. Pamula, P.G. Rouxhet, Bulk and surface chemical functionalities of type III PAN-based carbon fibres, *Carbon*, **41**, 2003, pp. 1905-1915.
- [12] S. Osbeck, R.H. Bradley, C. Liu, H. Idriss, S. Ward, Effect of an ultraviolet/ozone treatment on the surface texture and functional groups on polyacrylonitrile carbon fibres, *Carbon*, **49**, 2011, pp. 4322-4330.
- [13] Y. Yang, C.-X. Lu, X.-L. Su, G.-P. Wu, X.-K. Wang, Effect of nano-SiO<sub>2</sub> modified emulsion sizing on the interfacial adhesion of carbon fibers reinforced composites, *Materials Letters*, **61**, 2007, pp. 3601-3604.
- [14] F.H. Gojny, M.H.G. Wichmann, U. Köpke, B. Fiedler, K. Schulte, Carbon nanotube-reinforced epoxy-composites: enhanced stiffness and fracture toughness at low nanotube content, *Composites Science and Technology*, **64**, 2004, pp. 2363-2371.
- [15] S.-O. Lee, S.-H. Choi, S.H. Kwon, K.-Y. Rhee, S.-J. Park, Modification of surface functionality

- of multi-walled carbon nanotubes on fracture toughness of basalt fiber-reinforced composites, *Composites Part B: Engineering*, **79**, 2015, pp. 47-52.
- [16] R.J. Sager, P.J. Klein, D.C. Lagoudas, Q. Zhang, J. Liu, L. Dai, J.W. Baur, Effect of carbon nanotubes on the interfacial shear strength of T650 carbon fiber in an epoxy matrix, *Composites Science and Technology*, **69**, 2009, pp. 898-904.
- [17] V.P. Veedu, A. Cao, X. Li, K. Ma, C. Soldano, S. Kar, P.M. Ajayan, M.N. Ghasemi-Nejhad, Multifunctional composites using reinforced laminae with carbon-nanotube forests, *Nat Mater*, **5**, 2006, pp. 457-462.
- [18] J.J. Vilatela, D. Eder, Nanocarbon composites and hybrids in sustainability: a review, *ChemSusChem*, **5**, 2012, pp. 456-478.
- [19] T. Yokozeki, Y. Iwahori, S. Ishiwata, Matrix cracking behaviors in carbon fiber/epoxy laminates filled with cup-stacked carbon nanotubes (CSCNTs), *Composites Part A: Applied Science and Manufacturing*, **38**, 2007, pp. 917-924.
- [20] H.P.S. Abdul Khalil, P. Firoozian, I.O. Bakare, H.M. Akil, A.M. Noor, Exploring biomass based carbon black as filler in epoxy composites: Flexural and thermal properties, *Materials & Design*, **31**, 2010, pp. 3419-3425.
- [21] X. Zhang, X. Fan, C. Yan, H. Li, Y. Zhu, X. Li, L. Yu, Interfacial microstructure and properties of carbon fiber composites modified with graphene oxide, *ACS Appl Mater Interfaces*, **4**, 2012, pp. 1543-1552.
- [22] M. Sánchez, M. Campo, A. Jiménez-Suárez, A. Ureña, Effect of the carbon nanotube functionalization on flexural properties of multiscale carbon fiber/epoxy composites manufactured by VARIM, *Composites Part B: Engineering*, **45**, 2013, pp. 1613-1619.
- [23] T. Ogasawara, Y. Ishida, T. Kasai, Mechanical properties of carbon fiber/fullerene-dispersed epoxy composites, *Composites Science and Technology*, **69**, 2009, pp. 2002-2007.
- [24] A.K. Pathak, M. Borah, A. Gupta, T. Yokozeki, S.R. Dhakate, Improved mechanical properties of carbon fiber/graphene oxide-epoxy hybrid composites, *Composites Science & Technology*, **135**, 2016, pp. 28-38.
- [25] G. Vaganov, V. Yudin, J. Vuorinen, E. Molchanov, Influence of multiwalled carbon nanotubes on the processing behavior of epoxy powder compositions and on the mechanical properties of their fiber reinforced composites, *Polymer Composites*, **37**, 2016, pp. 2377-2383.
- [26] Y. Zhou, F. Pervin, V.K. Rangari, S. Jeelani, Influence of montmorillonite clay on the thermal and mechanical properties of conventional carbon fiber reinforced composites, *Journal of Materials Processing Technology*, **191**, 2007, pp. 347-351.
- [27] D. Banaś, A. Kubala-Kukuś, J. Braziewicz, U. Majewska, M. Pajek, J. Wudarczyk-Moćko, K. Czech, M. Garnuszek, P. Słomkiewicz, B. Szczepanik, Study of properties of chemically modified samples of halloysite mineral with X-ray fluorescence and X-ray powder diffraction methods, *Radiation Physics and Chemistry*, **93**, 2013, pp. 129-134.
- [28] X. Wu, C. Liu, H. Qi, X. Zhang, J. Dai, Q. Zhang, L. Zhang, Y. Wu, X. Peng, Synthesis and adsorption properties of halloysite/carbon nanocomposites and halloysite-derived carbon nanotubes, *Applied Clay Science*, **119**, 2016, pp. 284-293.
- [29] M. Li, H. Zang, J. Feng, Q. Yan, N. Yu, X. Shi, B. Cheng, Efficient conversion of chitosan into 5-hydroxymethylfurfural via hydrothermal synthesis in ionic liquids aqueous solution, *Polymer Degradation and Stability*, **121**, 2015, pp. 331-339.
- [30] P. Yuan, P.D. Southon, Z. Liu, M.E.R. Green, J.M. Hook, S.J. Antill, C.J. Kepert,

- Functionalization of Halloysite Clay Nanotubes by Grafting with  $\gamma$ -Aminopropyltriethoxysilane, *The Journal of Physical Chemistry C*, **112**, 2008, pp. 15742-15751.
- [31] C. Laginhas, J.M.V. Nabais, M.M. Titirici, Activated carbons with high nitrogen content by a combination of hydrothermal carbonization with activation, *Microporous and Mesoporous Materials*, **226**, 2016, pp. 125-132.
- [32] F.H. Chowdhury, M.V. Hosur, S. Jeelani, Studies on the flexural and thermomechanical properties of woven carbon/nanoclay-epoxy laminates, *Materials Science and Engineering: A*, **421**, 2006, pp. 298-306.
- [33] C.-K. Lam, H.-y. Cheung, K.-t. Lau, L.-m. Zhou, M.-w. Ho, D. Hui, Cluster size effect in hardness of nanoclay/epoxy composites, *Composites Part B: Engineering*, **36**, 2005, pp. 263-269.
- [34] J.F. Timmerman, B.S. Hayes, J.C. Seferis, Nanoclay reinforcement effects on the cryogenic microcracking of carbon fiber/epoxy composites, *Composites Science & Technology*, **62**, 2002, pp. 1249-1258.
- [35] N. Hameed, P.A. Sreekumar, B. Francis, W. Yang, S. Thomas, Morphology, dynamic mechanical and thermal studies on poly(styrene-co-acrylonitrile) modified epoxy resin/glass fibre composites, *Composites Part A: Applied Science and Manufacturing*, **38**, 2007, pp. 2422-2432.
- [36] B. De Vivo, P. Lamberti, G. Spinelli, V. Tucci, L. Guadagno, M. Raimondo, L. Vertuccio, V. Vittoria, Improvement of the electrical conductivity in multiphase epoxy-based MWCNT nanocomposites by means of an optimized clay content, *Composites Science and Technology*, **89**, 2013, pp. 69-76.
- [37] J.-H. Lee, K.Y. Rhee, S.J. Park, Silane modification of carbon nanotubes and its effects on the material properties of carbon/CNT/epoxy three-phase composites, *Composites Part A: Applied Science and Manufacturing*, **42**, 2011, pp. 478-483.
- [38] A.M. Díez-Pascual, B. Ashrafi, M. Naffakh, J.M. González-Domínguez, A. Johnston, B. Simard, M.T. Martínez, M.A. Gómez-Fatou, Influence of carbon nanotubes on the thermal, electrical and mechanical properties of poly(ether ether ketone)/glass fiber laminates, *Carbon*, **49**, 2011, pp. 2817-2833.
- [39] J. Folaranmi, Effect of Additives on the Thermal Conductivity of Clay, *Leonardo Journal of Sciences*, **8**, 2009.
- [40] S. Wang, J. Qiu, Enhancing thermal conductivity of glass fiber/polymer composites through carbon nanotubes incorporation, *Composites Part B: Engineering*, **41**, 2010, pp. 533-536.
- [41] W. Yuan, Q. Xiao, L. Li, T. Xu, Thermal conductivity of epoxy adhesive enhanced by hybrid graphene oxide/AlN particles, *Applied Thermal Engineering*, **106**, 2016, pp. 1067-1074.